The glycosphingolipid P_1 is an ovarian cancer-associated carbohydrate antigen involved in migration

F Jacob[*,1,2], M Anugraham[3], T Pochechueva[1], B W C Tse[2,4], S Alam[1], R Guertler[1,2], N V Bovin[5], A Fedier[1], N F Hacker[6], M E Huflejt[7], N Packer[3] and V A Heinzelmann-Schwarz[1,2,6]

[1]Gynecological Research Group, Department of Biomedicine, University Hospital Basel, University of Basel, Hebelstrasse 20, Basel 4031, Switzerland; [2]Ovarian Cancer Group, Adult Cancer Program, Lowy Cancer Research Centre, University of New South Wales, Prince of Wales Clinical School, Building C25 Kensington Campus, Sydney, NSW 2052, Australia; [3]Department of Chemistry and Biomolecular Sciences, Biomolecular Frontiers Research Centre, Faculty of Science, Macquarie University, Balaclava Road, North Ryde, Sydney, NSW 2109, Australia; [4]Australian Prostate Cancer Research Centre Queensland, Institute of Health and Biomedical Innovation, Queensland University of Technology, Translational Research Institute, Brisbane, QLD 4102, Australia; [5]Shemyakin-Ovchinnikov Institute of Bioorganic Chemistry, Russian Academy of Sciences, Ul. Miklukho-Maklaya, 16/10, Moscow 117997, Russian Federation; [6]Gynaecological Cancer Centre, Royal Hospital for Women, School of Women's and Children's Health, Barker Street, Randwick, NSW 2031, Australia and [7]Division of Thoracic Surgery and Thoracic Oncology, Department of Cardiothoracic Surgery, New York University School of Medicine, 550 First Avenue, New York, NY 10016, USA

Background: The level of plasma-derived naturally circulating anti-glycan antibodies (AGA) to P_1 trisaccharide has previously been shown to significantly discriminate between ovarian cancer patients and healthy women. Here we aim to identify the Ig class that causes this discrimination, to identify on cancer cells the corresponding P_1 antigen recognised by circulating anti-P_1 antibodies and to shed light into the possible function of this glycosphingolipid.

Methods: An independent Australian cohort was assessed for the presence of anti-P_1 IgG and IgM class antibodies using suspension array. Monoclonal and human derived anti-glycan antibodies were verified using three independent glycan-based immunoassays and flow cytometry-based inhibition assay. The P_1 antigen was detected by LC-MS/MS and flow cytometry. FACS-sorted cell lines were studied on the cellular migration by colorimetric assay and real-time measurement using xCELLigence system.

Results: Here we show in a second independent cohort ($n = 155$) that the discrimination of cancer patients is mediated by the IgM class of anti-P_1 antibodies ($P = 0.0002$). The presence of corresponding antigen P_1 and structurally related epitopes in fresh tissue specimens and cultured cancer cells is demonstrated. We further link the antibody and antigen (P_1) by showing that human naturally circulating and affinity-purified anti-P_1 IgM isolated from patients ascites can bind to naturally expressed P_1 on the cell surface of ovarian cancer cells. Cell-sorted IGROV1 was used to obtain two study subpopulations (P_1-high, 66.1%; and P_1-low, 33.3%) and observed that cells expressing high P_1-levels migrate significantly faster than those with low P_1-levels.

Conclusions: This is the first report showing that P_1 antigen, known to be expressed on erythrocytes only, is also present on ovarian cancer cells. This suggests that P_1 is a novel tumour-associated carbohydrate antigen recognised by the immune system in patients and may have a role in cell migration. The clinical value of our data may be both diagnostic and prognostic; patients with low anti-P_1 IgM antibodies present with a more aggressive phenotype and earlier relapse.

Glycosphingolipids (GSLs) have critical roles in embryonic development, signal transduction, cell signalling, apoptosis, receptor modulation, cell adhesion, growth and cell differentiation and carcinogenesis (Jarvis *et al*, 1996; Hakomori, 1998; Kasahara and Sanai, 1999). The presence of tumour-associated GSLs antigens have been observed in epithelial ovarian cancer (Pochechueva *et al*, 2012), which is the fifth most common cause of death from all cancers in women and the leading cause of death from gynaecological malignancies (Ozols, 2006).

Printed glycan array technology (a glycan-based discovery approach) previously demonstrated that naturally occurring anti-glycan antibodies (AGA) in plasma of ovarian cancer patients exhibited specificities towards synthetic P_1 trisaccharide. In our previous study, we have demonstrated using a printed glycan array that anti-P_1 antibodies can discriminate healthy controls from ovarian cancer patients (Jacob *et al*, 2012). This study (on a Swiss Discovery Cohort) showed that anti-P_1 antibodies of IgM, IgG and IgA together were significantly lower in ovarian cancer patients, thereby discriminating them from healthy controls. The predictive value of the printed glycan array was validated by two independent glycan-based immunoassays, ELISA and suspension array (Pochechueva *et al*, 2011b).

The P^k, P and P_1 carbohydrate antigens, commonly expressed on GSL, are members of the P blood group system that differ in their specificity based on their oligosaccharide sequences. In cancer, the globo (P^k and P) and neolacto (P_1) series are precursor GSL that give rise to well-known tumour-associated carbohydrate antigens, such as Forssman antigen (Hakomori *et al*, 1977; Taniguchi *et al*, 1981) and Globo H (Gilewski *et al*, 2001; Chang *et al*, 2008; Wang *et al*, 2008). High levels of P^k (Galα1-4Galβ1-4Glcβ1-1Ceramide; Gb3, CD77), P (GalNAcβ1-3Galα1-4Galβ1-4Glcβ1-1Ceramide; Gb4) and Globo H were described in the past (Wenk *et al*, 1994).

As shown previously, naturally occurring AGA to P_1 have the potential to be used diagnostically in plasma of ovarian cancer patients. However, it remains unknown whether P_1-bearing GSL are present on ovarian cancer cells and whether naturally occurring anti-P_1 antibodies to chemically synthesised carbohydrates in glycan-based immunoassays bind to these GSL antigens. To our knowledge, no published reports regarding the role of P_1 in malignant transformation, particularly in ovarian cancer, are available, and the molecular mechanisms underlying GSL expression on the cell surface, as well as its function, have yet to be elucidated. Therefore, this study aims (A) to determine the responsible naturally occurring AGA immunoglobulin class discriminating cancer from normal; (B) to determine whether the level of these antibodies are predictive of patient outcome; (C) to investigate whether the related P_1 glycan epitopes are present on cells isolated from ovarian cancer tissues as well as on ovarian cancer cell lines; (D) to compare the AGA profiles in ascites and matched plasma; (E) to compare monoclonal anti-P_1 antibodies produced in humans and affinity purified anti-P_1 antibodies isolated from ascites; and finally (F) to investigate the functional role of the P_1 antigen in ovarian cancer.

MATERIALS AND METHODS

Biospecimens. Two independent patient cohorts from two different continents were used for the experiments: (A) matched plasma and ascites from 11 serous FIGO stage III/IV cancer patients from the previously described Swiss Discovery Cohort (Jacob *et al*, 2012); (B) plasma from 155 Australian samples (Australian Validation Cohort) comprising healthy controls, borderline tumour and ovarian cancer patients. The Australian Validation Cohort was split into: (1) borderline tumours and

adenocarcinomas of the ovary, tube and peritoneum ('tumour group'), and (2) healthy control women ('control group'). Patients were either admitted with an adnexal mass to the Gynaecological Cancer Centre of the Royal Hospital for Women, Randwick, Australia or were seen as outpatients to the Hereditary Cancer Centre of The Prince of Wales Hospital, Randwick, Australia. All patients were prospectively included after giving informed consent in accordance with ethical regulations (Hunter Area Research Ethics 04/04/07/3.04; South Eastern Sydney Illawarra HREC/ AURED Ref:08/09/17/3.02). The processing of blood plasma samples was performed constantly on ice within 3 h after collection as previously described (Jacob *et al*, 2011a, 2012). All clinico-pathological data (Supplementary Table S1) such as FIGO stage and grade were incorporated in a specifically designed in-house database ('PEROV'), which was developed using Microsoft Access (Microsoft Corporation, Redmond, WA, USA). Diagnosis and histopathological features were independently re-evaluated by a pathologist specialised in gynaecological oncology (JS). Blood samples were stored in aliquots at $-80\,°C$.

Glycan-based immunoassays (printed glycan array, suspension array and ELISA). The printed glycan array was performed as previously described (Huflejt *et al*, 2009; Bovin *et al*, 2012; Jacob *et al*, 2012). AGA were detected by ImmunoPure goat anti-human IgA + IgG + IgM conjugated to long chain biotin (1 : 100, 'Combo', Pierce, Rockford, IL, USA). To detect the immunoglobulin class, developed printed glycan array slides were individually incubated with 1 : 50-diluted biotin-conjugated goat anti-human IgA, IgG or IgM (ZYMED Laboratories, Invitrogen, Carlsbad, CA, USA). The coupling procedures for end-biotinylated glycopolymers and antibody binding were described before (Pochechueva *et al*, 2011a, b). Experimental protocol was performed as described previously (Pochechueva *et al*, 2011b). Exceptions were made with respect to the use of goat anti-human IgG-R-PE or IgM-R-PE secondary antibodies (Southern Biotech Ass. Inc., Birmingham, AL, USA). ELISA was performed as described previously (Pochechueva *et al*, 2011b).

Extraction and identification of GSLs from cancer tissue samples and IGROV1 cell line. Fresh primary tissue samples (~ 100 mg) from a serous ovarian cancer and an endometrioid peritoneal cancer patient were collected to analyse glycolipids by negative ion electrospray ionisation mass spectrometry (LC-ESI-MS/MS). Detailed analysis of the procedure is described in Supplementary Information.

Affinity purification of anti-P_1 antibodies. Ascites fluid was collected from a late-stage serous ovarian cancer patient during primary surgery. The ascites was processed by centrifugation at $4\,°C$, 3000 **g** for 15 min. Supernatant was aliquoted and kept frozen at $-80\,°C$. Thawed ascites (50 ml) was filtered through a 0.22-μm filter (Millipore, Billerica, MA, USA) and diluted three times in PBS (pH 7.4). Glycan-polyacrylamide-Sepharose stored in 20% (v/v) ethanol was washed with 10 volumes 20% ethanol, 20 volumes milliQ water and equilibrated with 10 volumes of PBS. Preprocessed ascites affinity purified against Galα1-4Galβ1-4GlcNAcβ-polyacrylamide-Sepharose (P_1-PAA-Seph; 10 ml). A constant flow rate of 1 ml min^{-1} was controlled by the use of an auxiliary pump (Model EP-1 Econo Pump, Bio-Rad, Hercules, CA, USA). Protein content and buffer composition was recorded by UV at 280 nm and conductivity, respectively (BioLogic DuoFlow Workstation, Bio-Rad). The column was washed with PBS containing 0.05% (v/v) Tween 20, unplugged and stored overnight at $4\,°C$. The next day, the column was inserted back into the chromatography system and washed until no protein was detected anymore. Bound anti-P_1 antibodies were eluted using 0.2 M TrisOH (pH 10.2) and neutralised by 2.0 M Glycine HCl (pH 2.5). Eluted anti-P_1 antibodies were concentrated using the Amicon Ultra-0.5

centrifugal filter (Millipore), and their concentration was determined using spectrophotometrically at 280 nm.

Flow cytometry. GSL expression on the cell surface membranes was analysed by flow cytometry (CyAn ADP Analyzer, Beckman Coulter, Nyon, CH, USA) prior to antibody labelling. Unconjugated antibodies included anti-P$_1$ human IgM (clone P3NIL100; Immucor Gamma, Rödermark, Germany), anti-P$_1$ murine monoclonal IgM (clone OSK17; Immucor Gamma) and anti-Gb3 monoclonal IgG2b (CD77, P^k) (clone BGR23; Seikagaku Biobusiness Corporation, Tokyo, Japan). Biotin-conjugated antibodies included anti-human mouse IgM (BD Bioscience, Basel, Switzerland), rat anti-mouse IgM and rat anti-mouse IgG2b (BD Bioscience). Streptavidin conjugated to FITC (BD Bioscience) was used for fluorescence detection. Dead and apoptotic cells were separated from live cells using propidium iodide (BD Bioscience). Matching isotype monoclonal antibodies conjugated to FITC were used as controls (BD Bioscience). All investigated cell lines were gated individually to exclude debris, followed by single cell gating to remove dead cells and doublets. Data acquisition was performed using Summit v4.3 (CyAn ADP Analyzer, Beckman Coulter). Data analysis was performed using FlowJo v9 (Tree Star Inc., Ashland, OR, USA).

FACS sorting. IGROV1 cells were grown to 80% confluence, washed twice in PBS and harvested using non-enzymatic cell dissociation buffer (Sigma Aldrich, Buchs, Switzerland). Cells were then washed in PBS containing 1% FCS and resuspended to 10^6 cells ml^{-1}. Cell suspension (100 μl) was stained with human anti-P$_1$ IgM (BD Bioscience) as mentioned above and run on a BD FACS Vantage SE DiVa Cell Sorter (BD Bioscience). IGROV1 cell line was sorted using >90% and <10% fluorescence signal intensity for P$_1$-positive cells to receive P$_1$-high and P$_1$-low fractions, respectively.

Flow cytometry-based inhibition assay. Monoclonal human IgM antibody directed to P$_1$ (Immucor Gamma, Rödermark) was preincubated either with Sepharose-P$_1$-PAA or Sepharose-P^k-PAA (Lectinity Holdings, Moscow, Russia) in different amounts ranging from 0.015 μmol to 0.06 μmol for 60 min at RT. The supernatant was further processed as described in the flow cytometry section.

Colorimetric cell migration assay. Sub-confluent tumour cells were 'starved' from serum by incubation in serum-free media for 24 h, before harvesting using a non-enzymatic cell dissociation buffer (Sigma Aldrich, Buchs, Switzerland), washed twice and resuspended in serum-free media containing 5% (w/v) BSA. Tumour cells (7.5 × 10^5 in 300 μl) were loaded into cell culture inserts containing a polyethylene terephthalate membrane with 8-micron pores (Millipore). The inserts were assembled into 24-well plates with each well containing 700 μl of media with 10% supplemented with fetal calf serum, which was used as chemoattractant. After incubation for 18 h at 37 °C, the media in the interior of the insert was removed, and the entire insert was immersed in 400 μl of 0.2% crystal violet/10% ethanol for 20 min. The insert was washed several times in water, and the non-migrated cells in the interior of the insert were removed using a cotton-tip swab. After air-drying, five random areas of the inserts showing the migrated cells were photographed, and cell counts were performed. Colorimetric cell migration assay was performed three times.

In addition, parental IGROV1 cells were preincubated with 1% (w/v) BSA in PBS, the corresponding isotype control (ChromPure human IgM, Jackson ImmunoResearch Laboratories, Inc., MILAN Analytica AG, Rheinfelden, Switzerland) and human anti-P$_1$ IgM (clone P3NIL100), both antibodies in a final concentration of 500 μg ml^{-1}. After 1 h incubation, cells were processed according to previously described cell migration protocol.

MTT assay. Cultures were incubated with 500 μg ml^{-1} (final concentration) MTT dye (Sigma-Aldrich, Buchs, Switzerland) in PBS for 3 h, followed by removal of the medium and dissolution of the violet crystals in 200 μl of DMSO. The optical density (absorbance at 540 nm) was measured with a SynergyH1 Hybrid Reader (Biotek, Luzern, Switzerland). The data are given as absorbance at 540 nm, representing cell viability as a function of araC concentration. Each experiment was performed independently twice from multiple cultures.

Real-time cell migration analysis (xCELLigence). Real-time cell analysis (RTCA; xCELLigence System, Roche Diagnostics GmbH, Mannheim, Germany) was used to investigate cell migration in P$_1$-low and -high serous ovarian cancer IGROV1 cells in a label-free environment (Solly et al, 2004; Ke et al, 2011). Migration was examined on 16-transwell plates (Roche Diagnostics GmbH) with microelectrodes attached to the underside bottom of the membrane for impedance-based detection of the migrated cells. Prior to each experiment, cells were deprived of FCS over a period of 24 h. Initially, 160 μl 'chemoattractant' media (RPMI 1640 containing 10% FCS) and 50 μl RPMI 1640 containing 1% FCS was added to the lower and upper chambers, respectively. Sterile PBS was loaded into the evaporation trophs. CIM-16 plates were further prepared according to the manufacture's protocol. Background signals generated by the cell-free media were recorded. Cells were harvested using trypsin, counted and re-suspended in an appropriate volume of RPMI 1640 containing 1% FCS. Cells (100 000 cells per 100 μl medium) were seeded onto the upper chamber of the CIM-16 plate and allowed to settle onto the membrane. Cell-free media was used as negative control. Each experiment was performed two times in duplicates. The programmed signal detection for quantification of the cell index was measured every 15 min over a period of 30 h. In an independent migration assay, 5 μM of 1-beta-D-arabinofuranosylcytosine (araC; Sigma-Aldrich), a DNA polymerase inhibitor, was added to avoid possible effects on migration caused by cell proliferation.

Statistical analysis. Detailed statistical procedure applied is described in Supplementary Information.

RESULTS

IgM antibodies in plasma against P$_1$ trisaccharide are reduced in patients with tubal, peritoneal and ovarian cancer. In our previous study, the use of three glycan-based immunoassays (printed glycan array, ELISA and suspension array), detecting IgM, IgG and IgA together, revealed significant AGA interactions with the members of the P blood group system (Pochechueva et al, 2011a, b; Jacob et al, 2012). Overall, less AGA to P$_1$ trisaccharide (printed glycan array, ELISA and suspension array) and P^k (printed glycan array) were observed in the plasma of the cancer patient group compared with the control group (Pochechueva et al, 2011b; Jacob et al, 2012).

In this study, we investigated the levels of IgM and IgG AGA in the plasma of an independent Australian Validation Cohort ($n = 155$). The cohort consisted of a 'benign' control group (healthy controls and benign gynaecological conditions; $n = 81$) and a 'tumour' group (ovarian borderline tumours, ovarian, tubal and peritoneal cancers; $n = 74$) (Supplementary Table S1). Based on suspension array data, AGA to the P$_1$ trisaccharide belonged mainly to the IgM class (median, IQR; 9.948log(MFI), 9.351–10.090log(MFI)) in all the tested samples. Significantly lower IgM anti-P$_1$ antibody levels were observed in the blood plasma samples of the tumour as compared with the control group ($P = 0.0002$) (Figure 1A). The tumour group revealed 15/74 (20.3%) samples having lower AGA levels compared with the lowest control group sample. Logistic regression did not reveal any relationship between
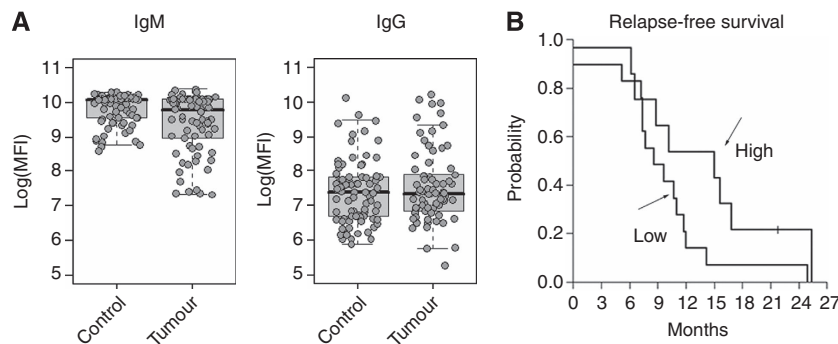
Figure 1. Significantly lower levels of anti-P$_1$ IgM in cancer patients in the Australian validation cohort ($n = 155$). (A) Box-and-whisker plots showing distribution of AGA levels of IgM and IgG to covalently attached P$_1$ trisaccharide using suspension array. Decreased AGA levels in cancer patients were observed for IgM. (B) Kaplan–Meier curve on relapse-free survival showing that patients with low antibody levels ($n = 33$; lower than median fluorescence signal) have slightly earlier relapse ($P = 0.055$) than those with high antibody levels ($n = 25$, higher than median fluorescence signal).

clinicopathological parameters and anti-P$_1$ IgM antibody signatures in the tumour group. In contrast to IgM, generally lower IgG antibody levels (median, IQR; 7.35log(MFI), 6.726–7.858log(MFI)) were observed. Both the control and tumour groups were similar in IgG AGA levels, with no significant difference in between both the groups ($P = 0.7248$, Figure 1A). We have compared various clinical parameters recorded along with collection of plasma samples for each patient. Statistical evaluation revealed a significant discrimination in FIGO stage of the non-mucinous cancer of ovary, tube and peritoneum group (FIGO Stage, non-mucinous cancer of the ovary, tube and peritoneum I/II vs III/IV, $P = 0.01773$, t-test). The remaining investigated clinical parameters were not significantly different in their anti-P$_1$ IgM antibody levels mentioning Grade (G1 vs G2/3, $P = 0.2883$; t-test) or tumour origin (ovary vs tube vs peritoneum, $P = 0.322$; ANOVA). An increasing age has previously been demonstrated to be associated with reduction of AGA in a cohort of 48 control plasma samples using glycopeptide arrays (Oyelaran et al, 2009). To investigate the influence of age on anti-P$_1$ antibodies (IgG and IgM), we have applied Pearson's correlation to suspension array data and found a moderate negative correlation (rho = -0.33, $P < 0.01$) in the entire cohort (mean age 56.4 (28–87) years). However, in contrast to the control group that showed a moderate negative correlation (rho = -0.37, $P < 0.01$), there was no correlation between age and anti-P$_1$ IgM levels in the tumour group (rho = -0.18, $P = 0.123$). This demonstrates that the reduction of anti-P$_1$ IgM is independent of age in the tumour group and further indicates an association of these lowered IgM levels with the disease. In contrast, we observed no correlation between age and anti-P$_1$ IgG levels in the control and tumour groups (Supplementary Figure S1). With regards to the risk of cancer recurrence (relapse-free survival), we observed that women with low IgM AGA levels to P$_1$ (lower than median fluorescence intensity, $n = 33$) were associated with a slightly higher risk ($P = 0.055$) of having an earlier recurrence than patients ($n = 25$) with higher levels of IgM anti-P$_1$ antibodies (hazard rate ratio 2.328, 95% CI 0.96–5.64) (Figure 1B). The disease-free survival analysis did not reveal any significant effect ($P = 0.605$).

**Identification of P blood group-related GSL in cancer tissues.** GSLs were extracted from fresh collected cancer tissues, and the glycans released from the glycolipids in the form of alditols (see 'Materials and methods') were analysed in the negative ion mode using LC-ESI-MS/MS to identify P blood group-related GSLs (Figure 2). The MS^2 spectra contained adequate information to facilitate the structural assignment of the glycans based on the fragment ions arising from various glycosidic and cross-ring cleavages, which were described previously (Domon and Costello, 1988).

The base peak chromatograms of the glycan alditols released from the GSLs extracted from serous ovarian (Figure 2A (a)) and peritoneal (Figure 2B (a)) cancer tissue showed several components. Globotriaosylceramide (Gb3, P^k) was detected as [M-H]$^{1-}$ m/z 505.3^{1-} at low intensities, and the extracted ion chromatogram (EIC) showed it eluting at 15.4 min (Figures 2A b(i) and B b(i)). The MS^2 spectra of the precursor ion at m/z 505.3^{1-} (Figure 2C (i)) showed prominent B- and C-type fragment ions (B$_1$ at m/z 161.1^{1-}, C$_1$ at m/z 179.2^{1-} and C$_2$ at m/z 341.1^{1-}) corresponding to a (Hex)$_3$ or Gal-Gal-Glc sequence of P$_k$. Characteristic cross ring fragment ions corresponding to ^{2,4}A$_2$ at m/z 221.2^{1-} and ^{0,2}A$_2$ at m/z 281.0^{1-} were also present in the spectrum, thereby confirming the presence of the 4-linked terminal Gal to the (Gal-Glc) disaccharide (Karlsson et al, 2010). A similar study indicated the absence of ^{0,2}A$_2$ fragment ion in the MS^2 spectrum of isoglobotriosylceramide (Galα1-3Galβ1-4Glcβ1) (Karlsson et al, 2010) while previous reports have also noted that this characteristic cross ring cleavage was useful in distinguishing between Type 1 (Galβ1-3GlcNAc) and Type 2 (Galβ1-4GlcNAc) chains commonly found in mucins (Chai et al, 2001; Robbe et al, 2004; Everest-Dass et al, 2012).

Globotetraosylceramide (P antigen, Gb4) was detected at [M-H]$^{1--}$ m/z 708.3^{1-} and the EIC showed it to elute at 17.0 min (Figures 2A c(ii) and B c(ii)). Despite appearing at low intensities, the MS^2 spectra of the precursor ion at m/z 708.3^{1-} (Figure 2C (ii)) was indicated by the B- and C-type fragment ions (B$_1$ at m/z 202.0^{1-}, B$_3$ at m/z 526.0^{1-}, C$_1$ at m/z 220.0^{1-} and C$_2$ at m/z 382.1^{1-}), which corresponded to the tetrasaccharide sequence, HexNAc$_1$Hex$_3$ or GalNAc-Gal-Gal-Glc of the P antigen. Several Y-ion fragments seen from the reducing-end were also identified at m/z 343.2^{1-} (Y$_2$) and m/z 505.2^{1-} (Y$_3$) while the diagnostic cross ring cleavages corresponding to ^{2,4}A$_3$ at m/z 424.1^{1-} and ^{0,2}A$_3$–H$_2$O at m/z 467.1^{1-} further confirmed the presence of 4-linked Gal to the internal Galβ1-4Glcβ1 of the Gb4 tetrasaccharide.

The pentasaccharide P$_1$, HexNAc$_1$Hex$_4$ or Gal-Gal-GlcNAc-Gal-Glc, was detected at [M-H]$^{1-}$ m/z 870.3^{1-} at 18.0 min in both tissue samples (Figures 2A d(iii) and B d(iii)). The glycosidic fragment ions occurring at m/z 305.1^{1-} (B$_2$–H$_2$O ion) and m/z 341.0^{1-} (C$_2$ ion) indicated the presence of the terminal Gal-Gal epitope while the Y-type fragment ions at m/z 546.2^{1-} (Y$_3$ ion) and a prominent m/z 708.2^{1-} (Y$_4$ ion) corresponded to the loss of the Gal-Gal epitope and terminal Gal, respectively, from the precursor ion, [M-H]$^{1-}$ m/z 870.3^{1-} (Figure 2C (iii)). Besides that, the prominent ^{2,4}x$_4$ fragment ion observed at m/z 648.3^{1-} in the MS^2 spectra was also characteristic of the terminal Gal residue linked via a 4-linkage to the Gal-GlcNAc-Gal-Glc tetrasaccharide. The cross ring cleavage at ^{0,2}A$_3$–H$_2$O at m/z 425.1^{1-} and the
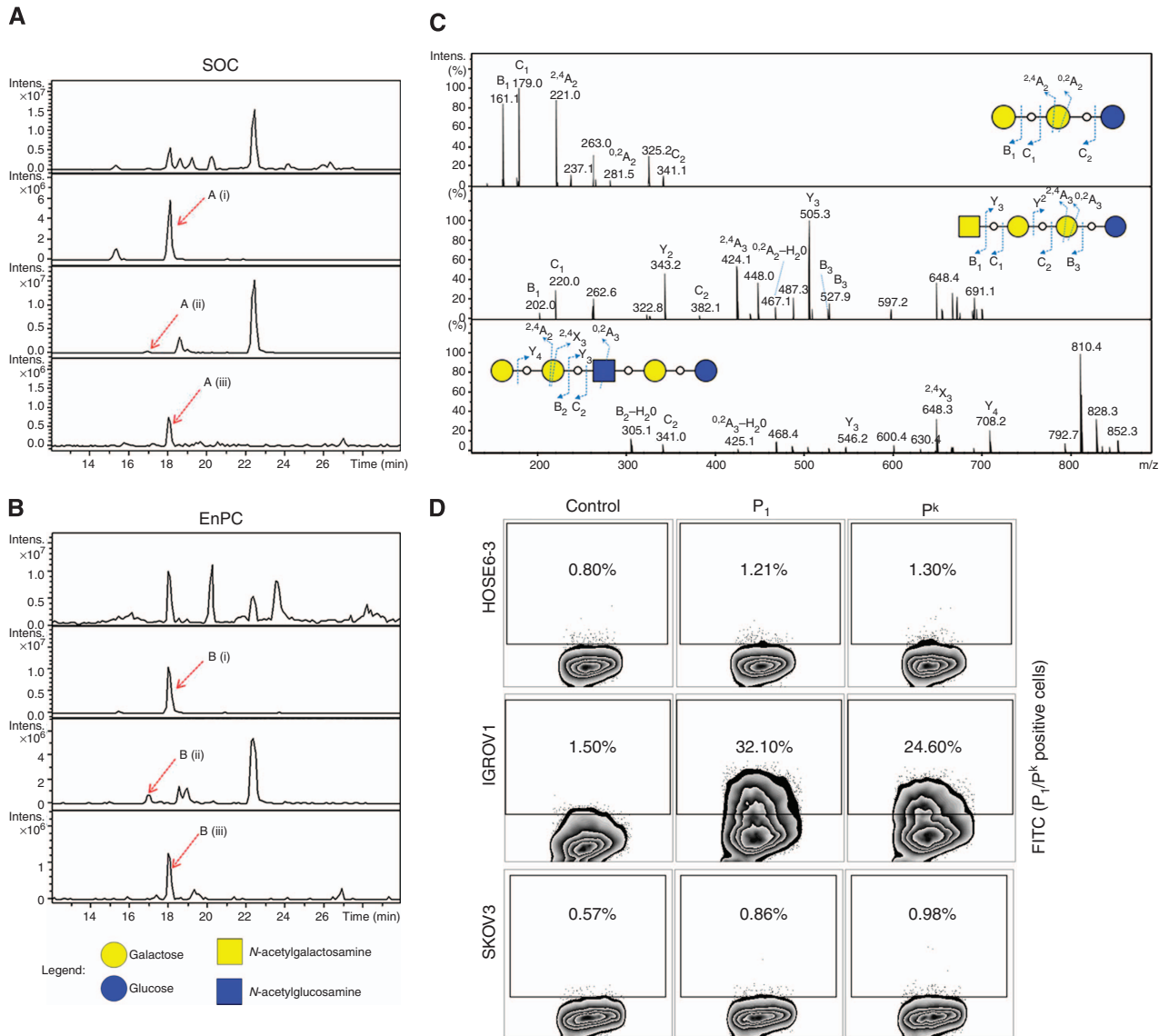
Figure 2. P$_1$ is expressed on cancer tissue cells. (A, B) Base peak chromatograms shown for serous ovarian cancer (A (a)) and endometrioid peritoneal cancer tissue (B (a)). Selected mass peaks (red arrow) corresponding to the composition of the P^k trisaccharide (Hex$_3$) (A and B b(i); m/z 505.3^{1-}), P tetrasaccharide (Hex$_3$HexNAc$_1$) (A and B c (ii); m/z 708.3^{1-}), and P$_1$ pentasaccharide (Hex$_4$HexNAc$_1$) (A and B d(iii); m/z 870.3^{1-}) are represented as an extracted ion chromatogram (EIC). (C) MS^2 spectrum of P^k trisaccharide (Galα1-4Galβ1-4Glcβ1) (i), P tetrasaccharide (GalNAcβ1-3Galα1-4Galβ1-4Glcβ1) (ii) and P$_1$ pentasaccharide (Galα1-4Galβ1-4GlcNAcβ1-3Galβ1-4Glcβ1) (iii). (D) Representative flow cytometry results shown as contour plots with outliers demonstrate P$_1$ and P^k negative cell lines HOSE6-3 and SKOV3. IGROV1 was detected positive with IgMs for both P$_1$ and P^k. Representative contour plots showing P$_1$ and P^k expression (FITC; ordinate) and forward scatter (FSC; abscissa). Given percentage corresponds to P$_1$/P^k-positive cells.

absence of the $^{0,2}A_4$ at m/z 646.1^{1-} further demonstrates the 4-substitution of the GlcNAc residue and the 3-substitution of the internal Gal and thus tentatively identified this compound as Galα1–4Galβ1-4GlcNAcβ1–3Galβ1-4Glc, the P$_1$ antigen. The three P blood group antigens were thus shown to be expressed on the GSL of serous ovarian and peritoneal cancer tissues. There was insufficient tubal cancer tissue sample to identify the presence of these antigens.

P$_1$ is expressed on IGROV1 cell surface. As IgMs were raised against the P$_1$ antigen in plasma from all types of ovarian cancer patients, and the P$_1$ (P^k and P) antigens were found to be expressed on the GSL extracted from the cancer tissue of these patients, we established an experimental cell culture model for the investigation into the functional role of P$_1$. Our panel of immortal cell lines, including human ovarian surface epithelial cells (HOSE6-3 and

HOSE17-1) and various ovarian cancer cell lines ($n = 6$), were profiled for P$_1$ and P^k expression using flow cytometry (Figure 2D). Serous ovarian cancer cell line IGROV1 was heterogenic for P$_1$ expression (mean 34.1% ranging from 22.8% to 52.8%) based on human anti-P$_1$ IgM (clone P3NIL100) antibody. The second antibody used in this study, monoclonal murine anti-P$_1$ IgM (clone OSK17), confirmed P$_1$ expression on IGROV1 (mean 22.3% ranging from 22.0% to 33.6%). IGROV1 cells were also positive for P^k (mean 33.6% ranging from 12.0% to 54.0%). The normal control cell line HOSE6-3 was negative for both P$_1$ and P^k as were the remaining ovarian cancer cell lines ($n = 5$).

To verify the presence of P$_1$ on IGROV1 cell line, we isolated GSLs from this cell line and analysed the released glycan alditols using negative ion mode LC-ESI-MS/MS. The P$_1$ pentasaccharide at m/z 870.3^{1-} was shown to elute at 20.3 min, and the MS^2 spectra consisted of B$_2$ (m/z 323.1^{1-}), Y$_3$ (m/z 546.3^{1--}) and Y$_4$

(m/z 708.3^{1-}) fragment ions, which corresponded to the Gal-Gal-GlcNAc-Gal-Glc sequence. The terminal Galα1–4Gal linkage was also determined by the cross ring fragment ion at $^{2,4}x_4$ fragment ion observed at m/z 648.3^{1-} (Supplementary Figure S2).

Monoclonal anti-P$_1$ IgM bind IGROV1 cells. Both P$_1$ and P^k share terminal disaccharide structure of composition Galα1–4Galβ1–4Glc(NAc). The monoclonal antibody to P$_1$ (clone P3NIL100) was used in a flow cytometry-based inhibition assay. Sepharose conjugated PAA-lactose, -N-acetyllactoseamine (Lac-NAc), -P$_1$ trisaccharide, -P^k was incubated with the monoclonal antibody to P$_1$ before immunostaining of IGROV1 cells to observe the degree of inhibition of IgM antibody binding to the expressed P$_1$ on IGROV1 cell surface. In this experiment, repeated three times, flow cytometry of 52.8% P$_1$-positive IGROV1 cells revealed complete inhibition of monoclonal anti-P$_1$ antibody by preincubating with 0.015 μmol P$_1$ glycoabsorbents (0.04%). In contrast, less reduction (28.3% by 0.06 μmol P^k) of bound anti-P$_1$ antibodies to IGROV1 cells was observed in case of P^k glycoabsorbent (Figure 3). Anti-P$_1$ antibodies were only slightly inhibited by preincubation with glycoadsorbents Lactose (0.06 μmol; 46.8%) and LacNAc (0.06 μmol, 44.8%). This clearly demonstrates that IGROV1 cells express P$_1$ on their cell surface, and monoclonal antibody to P$_1$ shows clearly higher affinity to P$_1$ compared with P^k. It also demonstrates specifically that galactose α1–4 link is required for antibody binding and that lactose and LacNAc are not primarily epitopes of P$_1$.

Anti-glycan antibodies levels are similar in ascites and blood plasma. To determine whether anti-tumour antibodies were expressed in ascites as well as plasma of patients, we investigated the presence and distribution of AGA in matched ascites and blood plasma samples ($n = 11$ patients) for IgA, IgG and IgM together

and separately using the printed glycan array. This was also done for epitope mapping of ascites-derived human anti-P$_1$ antibodies.

We detected a broad spectrum of AGA in both plasma and ascites (Figure 4). The fluorescence scan of the binding to the immobilised glycans on the array showed high amplitude of AGA in ascites of IgG, IgM and IgA in both 50 μM and 10 μM glycan-printed arrays (Supplementary Figure S3). We observed the highest median relative fluorescence signals in ascites (median, 32.75 × 10^4 RFU) and in plasma (43.33 × 10^4 RFU) for anti-glycan IgM antibodies. Anti-glycan IgG antibodies showed lower interaction with the glycans (ascites (8.11 × 10^4 RFU), plasma (9.80 × 10^4 RFU) as well as anti-glycan IgA (ascites (8.8 × 10^4 RFU), plasma (10.4 × 10^4 RFU)). Different levels of AGA to P$_1$ trisaccharide were detected in all the tested ascites and plasma samples (Figure 4). Highest binding to P$_1$ was observed for IgM (ascites (18.1 × 10^4 RFU), plasma (14.3 × 10^4 RFU)) compared with IgG and IgA.

Matched ascites and plasma AGA signals were not dependent on the volume of patient's ascites. Based on raw data sets of 50 μM printed glycan arrays, strong correlation between matched ascites and blood plasma samples was observed (Figure 4): IgA + IgG + IgM (CCC = 0.889), IgA (CCC = 0.888), IgG (CCC = 0.961), and IgM (CCC = 0.950). Correlations were similar for 10 μM printed glycans. This demonstrates that detected AGA levels were independent of the volume of ascites.

Naturally occurring anti-P$_1$ antibodies in ascites bind to cancer cells expressing P$_1$ on their cell surface. The results achieved from the above experiments demonstrated that (A) anti-P$_1$ antibodies detected by glycan-based immunoassays are reduced in plasma of cancer patients, (B) P blood group-related glycans are detectable in tissue samples of cancer patients, (C) IGROV1
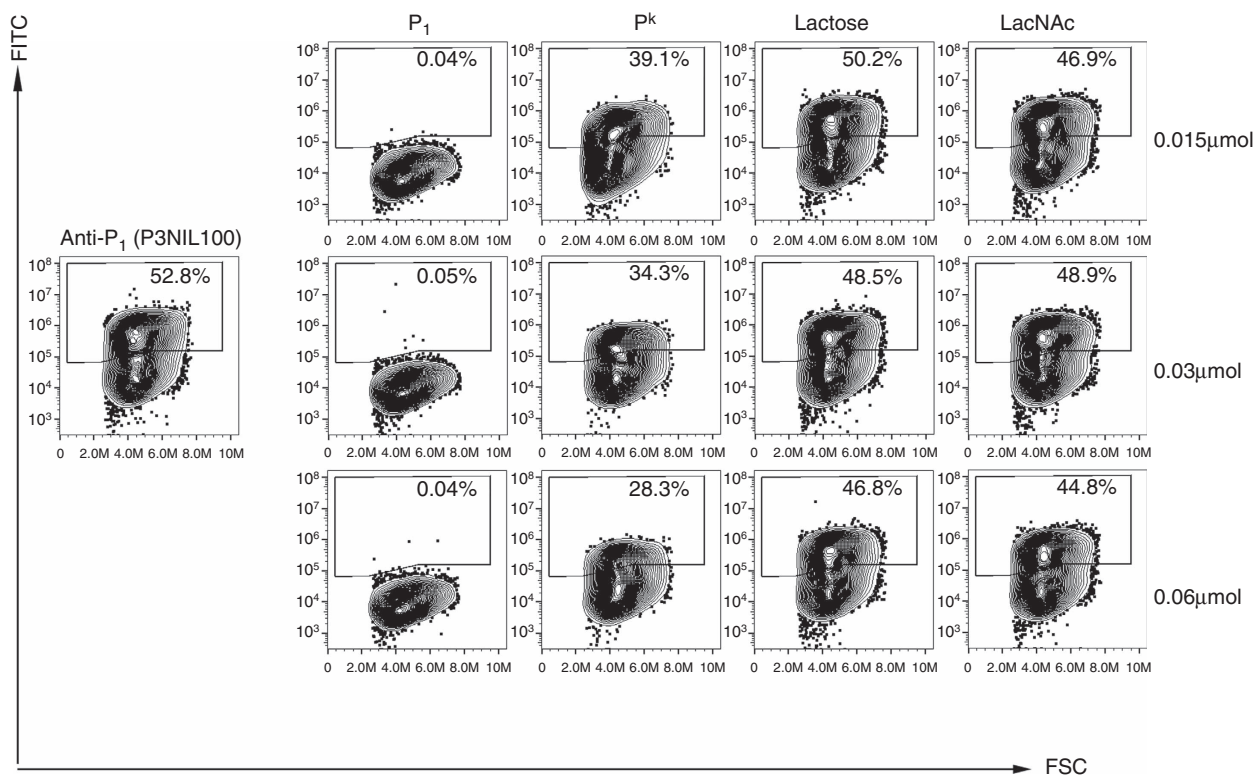
Figure 3. Monoclonal anti-P$_1$ IgM bind specifically to P$_1$. Monoclonal anti-P$_1$ antibody (P3NIL100, positive control) was incubated with different glycan amounts (0.015–0.06 μmol) prior to flow cytometric measurement of binding to IGROV1 cells. Glycoconjugates Sepharose-PAA (-Lactose, -LacNAc, -P$_1$, -P^k) were applied to test specificity of antibodies to P$_1$ by testing the inhibition of binding of the anti-P$_1$ antibody. Representative contour plots out of three independent experiments showing P$_1$ expression (FITC; ordinate) and forward scatter (FSC; abscissa). Complete inhibition is shown by increasing Seph-PAA-P$_1$ amount with only minor inhibition of anti-P$_1$ antibodies using Seph-PAA-P^k.
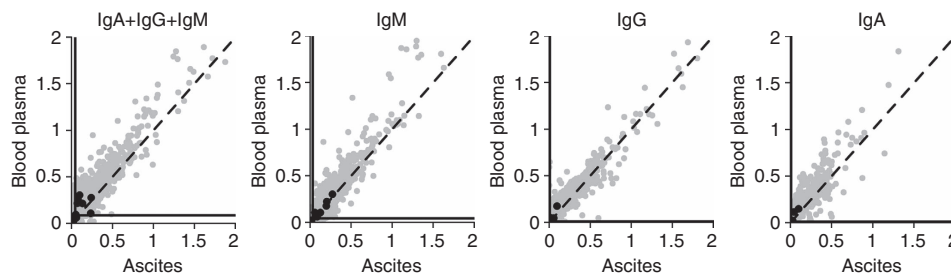
Figure 4. Ascites and blood plasma from cancer patients contain comparable levels of anti-glycan antibodies independent of immunoglobulin class and volume of ascites. Matched ascites and blood plasma samples ($n = 11$) were profiled for binding of IgA + IgG + IgM ($n = 22$ printed glycan array slides) and independently for IgA ($n = 22$), IgG ($n = 22$) and IgM ($n = 22$) to printed glycan array slides. One scatterplot represents signals for 11 patients each with ascites and blood plasma. AGA to P$_1$ trisaccharide are highlighted in black. Median signal intensity over all signals calculated for ascites and plasma are shown by horizontal and vertical solid lines, respectively. Antibody signals (RFU $\times 10^6$) are shown on ascites and blood plasma axis. Cutoff (5%) separating background signals from real AGA binding are indicated by a solid line for ascites and plasma in the same scatterplot.

ovarian cancer cell line was found to express P$_1$ on its cell surface among all the tested cell lines and (D) profiled ascites contained AGA to P$_1$ trisaccharide. Therefore the following series of experiments were aimed to investigate whether IgM antibodies derived from ascites bind to IGROV1 and in particular to P$_1$ presented on its cell surface in the same way as the plasma-derived autoantibodies.

We investigated AGA to P$_1$ trisaccharide from an ascites sample of a late-stage serous ovarian cancer patient. The ascites fluid was first applied to the IGROV1 cell line in a 1 : 3 dilution, in which 24.3% of cells were stained positive with ascites-derived IgM antibodies (Figure 5A). Based on this result, we proceeded to affinity purify antibodies bound specifically to P$_1$ trisaccharide conjugated to sepharose beads. Affinity-purified proteins yielded a maximum amount of IgM of 24 μg after concentration. Detection of purified anti-P$_1$ antibodies of class IgM revealed binding to P$_1$-expressing IGROV1 (15.1%) (Figure 5A). In contrast, the ovarian cancer cell line SKOV3, negative for P$_1$ and P^k expression, had a positive staining of only 0.29% using the purified IgM-P$_1$ antibodies. This demonstrates for the first time that ascites-derived AGA directed to P$_1$ trisaccharide also bind to naturally expressed P$_1$ on cell surface of ovarian cancer cells. In the following ELISA experiment on purified IgM-P$_1$ antibodies (Figure 5B), higher values for IgM (OD$_{450\,nm}$ = mean $3.23 \pm$ s.d. 0.08) compared with IgG (OD$_{450\,nm}$ = 1.08 ± 0.02) were observed.

Next, we investigated whether purified IgM-P$_1$ antibodies bind to glycan structures other than P$_1$ (potential cross-reactivity). ELISA to a limited number of glycoconjugates revealed in the case of IgM specific binding to P$_1$ trisaccharide, with cross-reactivity to Galα1-3GalNAc and Galα1-4GlcNAc (Figure 5B). Suspension and printed glycan array were additionally utilised to study the cross-reactivity to broader range of glycan structures, other than P$_1$. In suspension array, the binding of ascites-derived anti-P$_1$ antibodies to P$_1$, P^k, Le^y and α-rhamnose was tested. No preferential binding was observed comparing P$_1$ and P^k (P$_1$ 4.11log(MFI); P^k 4.24log(MFI), IgM class). In contrast, Le^y and α-rhamnose coupled beads revealed only minor binding. In the printed glycan array (Figure 5C), we applied a threshold of 5% to the highest median fluorescence signal (19 443 RFU; Galα1–4Galβ1–4Glc-sp3) to eliminate potentially unspecific binding as described previously (Huflejt et al, 2009). We identified that affinity-purified IgM-P$_1$ antibodies bound to P blood group-related structures as the top 10 glycans (Supplementary Table S2). Most of the identified low-affinity binding to glycan structures had substructures of the P$_1$ antigen such as Galβ1-4Glc(NAc) with 63.0% and Galα1-4Galβ with 22.2% binding reactivity (Supplementary Table S2). This demonstrates that affinity-purified IgM-P$_1$ antibodies preferentially bound to both P^k and P$_1$ trisaccharide.

P$_1$ expression leads to elevated migration rate in ovarian cancer cells. GSLs on the cell surface are described to have several functions in cellular processes, such as pathogen recognition, angiogenesis, cell motility and cell migration (Panjwani et al, 1995; Todeschini et al, 2008; Hakomori, 2010). Migration is a common feature in cancer cells, and therefore we investigated whether or not the presence of P$_1$ affects cell migration by using a flow cytometry-based cell sorting of IGROV1 cells to separate P$_1$-high-from P$_1$-low-expressing subpopulations. After further sub-cultivation, P$_1$ expression in P$_1$-low IGROV1 cells was determined by murine monoclonal anti-P$_1$ IgM (OSK17; 18%) or human anti-P$_1$ IgM (P3NIL100; 33.3%). In contrast, P$_1$-high-expressing IGROV1 cells were 50.0% and 66.1% positive for P$_1$, respectively, for these antibodies (Figure 6A).

Utilising these P$_1$-sorted cell lines, we hypothesised that the presence of P$_1$ affects cell migration. Significantly higher migration was detected in P$_1$-high-expessing when compared with P$_1$-low-expressing IGROV1 cells after an 18 h incubation period ($P = 0.0006$) (Figure 6B), as shown by colorimetric cell migration assay. In addition to end-point migration assay, real-time and label-free measurement of P$_1$-sorted IGROV1 cells was performed using the xCELLigence system. A number of 100 000 cells was seeded into each well of the upper chamber, and migration through the microporous membrane were recorded as cell index. IGROV1 cells with higher P$_1$ were significantly faster after 20 h ($P = 0.035$) than low P$_1$ cells. Longer incubation periods resulted in no difference between both subpopulations (30 h; $P = 0.1337$, 40 h; $P = 1$; Figure 6C). To avoid the influence of potentially elevated proliferation effects, 5 μM cytosine arabinoside (araC) was added to the cell culture (Supplementary Figure S4). In concordance with results on the colorimetric cell migration assay and observations on initial xCELLigence experiment, cells with elevated P$_1$ displayed high basal migratory activity as indicated by the increases in cell index values, reflecting the number of migrating cells. In contrast, P$_1$-low-expressing cells failed to migrate under experimental conditions. With regard to migratory kinetics, P$_1$-high-expressing cells migrated rapidly and demonstrated elevated (4.7-fold) cell index of 0.3434 ± 0.054 (mean $\pm$ s.d.) as compared with P$_1$-low-expressing cells (0.0726 ± 0.029; $P = 0.004$, CI 0.1–0.45). This difference remained constant throughout the 40 h time course experiment (20 h–3.6-fold ($P < 0.001$, CI 0.32–0.66); 30 h–3.6-fold ($P < 0.001$, CI 0.40–0.75); 40 h–4.6-fold ($P < 0.001$, CI 0.49–0.84); Figure 6C). These findings demonstrate that ovarian cancer cells expressing P$_1$ on their cell surface migrate faster compared with low-P$_1$-expressing cells originated from the same parental cell line.

In order to confirm that P$_1$ is involved in cell migration, we performed the colorimetric cell migration assay with anti-P$_1$ IgM-pretreated IGROV1 cells. The results (Figure 6D) showed that the
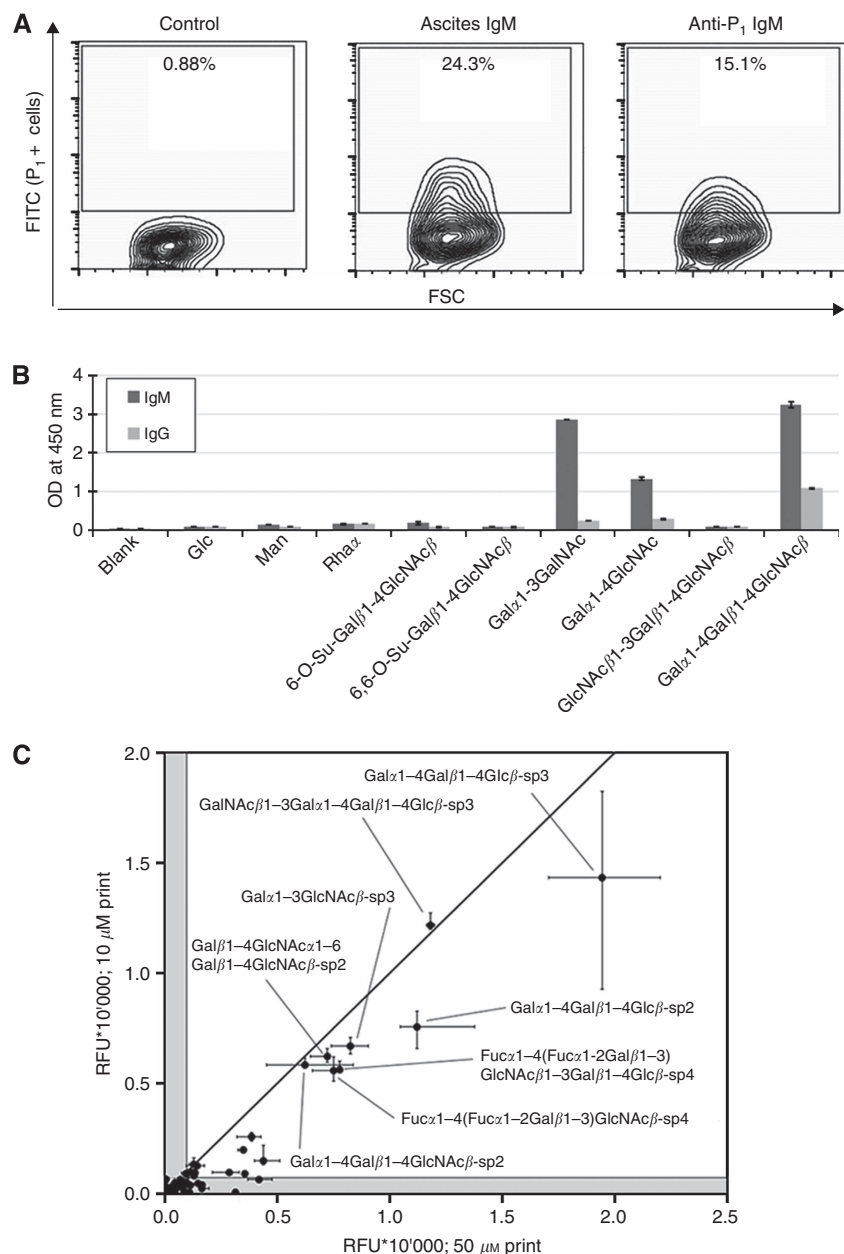
Figure 5. Human ascites-derived affinity-purified anti-P_1 antibodies bind to IGROV1 cells. (**A**) Flow cytometry-based contour plots demonstrate the presence of IgM antibodies in ascites (1 : 3 diluted in PBS) bound to IGROV1 cells (ascites IgM, 24.3%) compared with unstained sample (control). Affinity-purified anti-P_1 IgM (1 : 20) bound to IGROV1 cells (15.1% of P_1-positive cells). (**B**) Representative ELISA demonstrating the cross-reactivity of affinity-purified anti-P_1 antibodies of class IgM (dark grey) and IgG (light grey) to investigated glycans linked to PAA. (**C**) Printed glycan array data (scatterplot for 50 μM vs 10 μM saccharide prints) showing cross-reactivity to glycans sharing related carbohydrate structures. Grey area indicates unspecific binding of AGA as determined by 5% threshold. Inter-quartile range is shown for each glycan horizontally and vertically for 50 μM and 10 μM, respectively.

percentage of migrated cells was significantly lower (reduction by 64%; $P < 0.001$) in cultures preincubated with the anti-P_1 IgM antibody. Pretreatment with the respective IgM isotype control did not affect the migration of IGROV1 cells.

DISCUSSION

Unlike P^k, which has been extensively studied in the areas of verotoxin-mediated cytotoxicity, human immunodeficiency virus infection, immunology and epithelial carcinogenesis, there is, to our knowledge, no published study of P_1 and its potential presence, immunogenicity and its functional role in oncogenesis. Using glycan-based immunoassays, we have previously demonstrated that naturally occurring AGA significantly distinguish healthy controls from ovarian cancer patients (Pochechueva *et al*, 2011b; Jacob *et al*, 2012). The present study demonstrates that: (A) an unknown subpopulation of cancer patients show reduced levels of anti-P_1 IgM antibodies in an extended and independent cohort from another continent (Australian Validation Cohort), (B) P^k, P and P_1 carbohydrate antigens are detectable in cancer tissue as well as on the cell surface of cultured ovarian cancer cells, (C) ascites contains similar anti-glycan IgM-P_1 antibody levels compared with blood plasma independent of its volume at the primary diagnosis, (D) naturally occurring AGA of IgM class derived from ascites of a
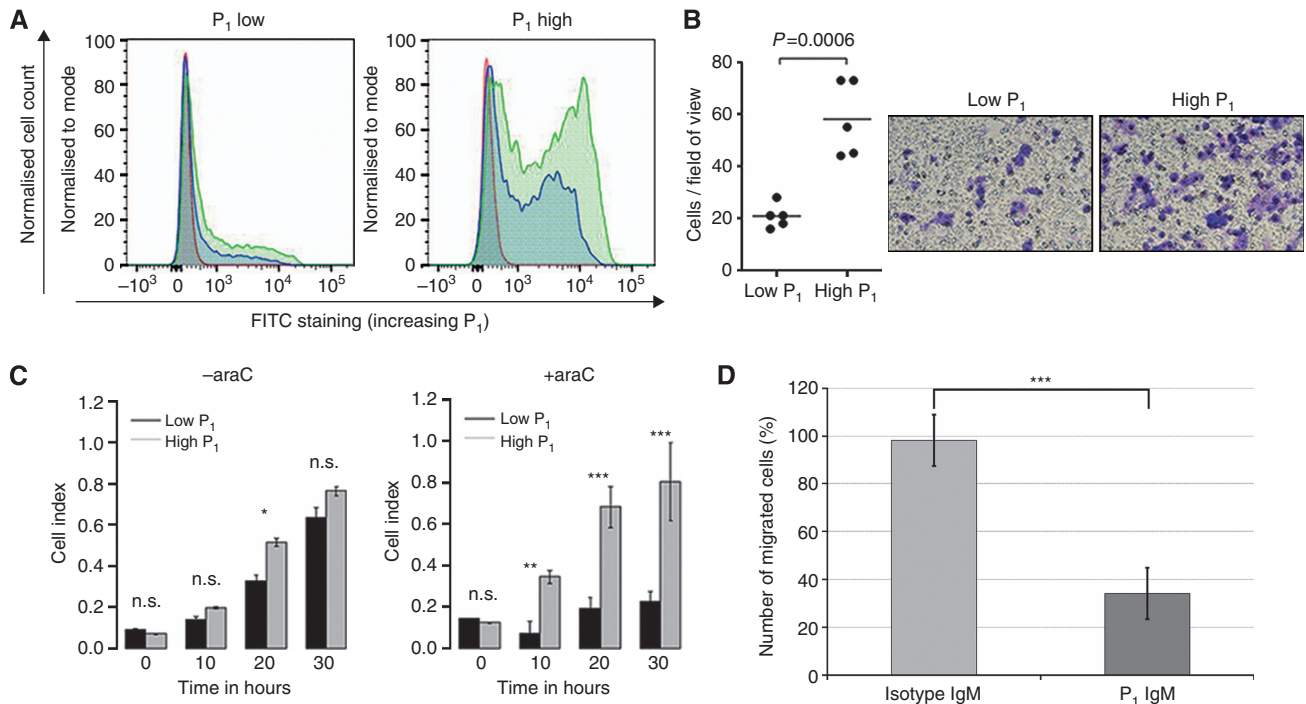
Figure 6. Elevated P$_1$ expression results in increased migration rate. (A) FACS-sorted subpopulations of P$_1$-low- and -high-expressing IGROV1 cells. Representative histograms showing P$_1$ expression (abscissa) on cell-sorted IGROV1 cells to normalised cell count (ordinate). P$_1$ distribution for unstained controls (red), P$_1$-positivity P3NIL100 antibody (green) and OSK17 antibody (blue). (B) Colorimetric cell migration assay showing enhanced migratory ability of IGROV1 cells expressing high compared with low levels of P$_1$. Stained cells counted in five fields and averaged. Representative image of cell sorted subpopulations of migrated cells (stained violet) after 18 h. (C) RTCA assay for P$_1$-sorted IGROV1 cells showing the migrated cells (cell index) in bar graphs at the time points 0 h, 10 h, 20 h and 30 h. Left bar graph shows RTCA experiment without araC, right bar graph with araC as proliferation inhibitor. Representative figure out of two independent experiments. (D) Bar chart showing the inhibition of cell migration of human IGROV1 cells incubated with anti-P$_1$ IgM compared with corresponding incubation with IgM isotype control. Number of migrated cells was normalised to control. Not significant (NS); *$P < 0.05$, **$P < 0.01$, ***$P < 0.001$.

ovarian cancer patient bind to naturally expressed and chemically synthesised P$_1$ on glycan arrays, and (E) the presence of P$_1$ on ovarian cancer cultured IGROV1 cells leads to enhanced migration.

Our results demonstrate that the significantly lower anti-P$_1$ antibody levels observed in cancer patients were primarily due to the reduction of IgM but not IgG antibodies. This is in full concordance with the literature on the IgM type anti-Thomsen Friedenreich antibodies (Desai et al, 1995) and anti-Lewis C antibodies in breast cancer (Bovin, 2013). A very recently published work demonstrated significantly reduced human IgM antibodies to another GSL (N-glycolylneuraminyl)-lactosylceramide (NeuGcGM3) in non-small cell lung cancer patients (Rodriguez-Zhurbenko et al, 2013). Therefore we can assume that IgM class of naturally occurring AGA was able to discriminate between cancer and healthy controls. Natural IgM antibodies belong to the innate immune system and are primarily produced by B1 or CD5+ cells (Boes, 2000; Martin and Kearney, 2001; Viau and Zouali, 2005). As part of the natural immunity, the binding of IgM to conserved carbohydrate structures acts as a first barrier to all invasive particles ('external') and alterations on proteins and lipids within an organism ('internal') (Vollmers and Brandlein, 2007). To date, several human monoclonal antibodies directed to tumour-associated carbohydrate antigens have been isolated. For instance, the monoclonal IgM antibody, SAM-6, specific for cancerous tissue was first derived from a gastric cancer patient (Pohle et al, 2004). Later, it was found that the receptor for SAM-6 is a tumour-specific O-linked carbohydrate epitope on GRP78, a central regulator of endoplasmatic reticulum in protein folding (Li and Lee, 2006). PAM-1, another monoclonal IgM antibody, binds to a tumour-specific N-linked carbohydrate epitope, a posttranslational modification on cysteine-rich fibroblast growth

factor receptor, CFR-1. This antibody also inhibited tumour growth in vitro and in animal model systems by inducing apoptosis (Brandlein et al, 2003, 2004a, b). Consistent with the findings of Vollmers and colleagues regarding SAM-6 and PAM-1, our observation based on hierarchical clustering indicates that AGA preferentially bind to substructures of the glycan epitope (Jacob et al, 2012). Besides that the decrease of AGA mainly of the IgM class in gynaecological cancer patients (Jacob et al, 2012) also points to an involvement of naturally occurring IgM autoantibodies, which recognise GSL structures. We further propose that Galα1-4Galβ1-4Glc(NAc) (present in P, P^k and P$_1$ antigens) are a result of malignant transformation and could serve as an 'internal' epitope on GSLs that is recognised by naturally circulating anti-glycan IgM antibodies.

The observation of lower levels of anti-P$_1$ IgM compared with anti-P$_1$ IgG in cancer patients is very intriguing, and although exploring the underlying mechanisms was beyond the scope of the study, we speculate on a number of possibilities. The elevated presence of corresponding antigens on cancer cells, in our case P$_1$ GSL, may be bound by circulating anti-P$_1$ IgM and therefore no longer be freely floating in the plasma and ascites. Another potential mechanism may be tumour-induced immune suppression. It is known that ovarian cancers employ a range of strategies, such as secretion of immunosuppressive cytokines, to facilitate their escape from immune destruction (Lavoue et al, 2013). It is possible that this may lead to reduced antibody production against cancer-associated antigens, for example, P$_1$, conferring a survival advantage to cancer cells. The antibody repertoire in cancer patients would therefore be different. Another possible mechanism is the occupation of anti-P$_1$ IgMs by cancer cells (including circulating tumour cells) by virtue of their surface expression of

P$_1$, leading to a reduction in the amount of unbound antibody in plasma and/or ascites. The formation of immune complexes consisting of P$_1$ antigen shed from cancer cells, and anti-P$_1$ IgMs, may further contribute to this reduction. A prominent example in the literature for the formation of circulating immune complexes consisting of Lewis x and antibodies has been shown in *Helicobacter pylori*-infected human (Chmiela *et al*, 1998). With regards to no change being observed in the anti-P$_1$ IgG levels, we expected differences preferentially in the case of IgM rather than of IgG as glycan-based antigens are T-cell-independent antigens and are recognised by the innate immune system.

Our mass spectrometry results demonstrated that these P$_1$, P^k and P antigens are expressed on ovarian and peritoneal cancer tissues. The functional role of the GSL that carry these structures in carcinogenesis is poorly understood, especially in the case of P$_1$ and P. It was recently described that a monoclonal anti-P^k antibody (E3E2) inhibited angiogenesis and tumour development (Desselle *et al*, 2012). Enhanced expression of P^k has also been shown to cause doxorubicin resistance in breast cancer cells (Gupta *et al*, 2012). Cisplatin-resistant pleural mesothelioma cells were shown to be sensitised to cisplatin by the addition of sub-toxic concentrations of Verotoxin 1 (Johansson *et al*, 2010). In addition, we also demonstrate that P$_1$ and P^k antigens are also present on the surface of the IGROV1 serous ovarian cancer cells. IGROV1 is, therefore, to the best of our knowledge, the only immortal cell line from several investigated that expresses P$_1$. Using monoclonal antibodies against P$_1$, only minor cross-reactivity to other glycan structures was observed in glycan-based immunoassays (not shown). Furthermore, based on the flow cytometry inhibition assay using IGROV1 cells as an investigative model, the specificity of monoclonal antibodies to P$_1$ as shown by the full saturation of anti-P$_1$ antibodies by inhibition with 0.06 μmol glycan on sepharose beads indicates that IGROV1 expresses P$_1$ on the cell surface.

Serous pelvic masses commonly present with malignant ascites, a plasma–protein-rich intraperitoneal exudate of up to several litres. Several pathophysiological mechanisms are necessary for malignant ascites occur: (a) decreased lymphatic ascites absorption, (b) increased capillary permeability, (c) increased overall capillary membrane-surface area available for filtration, and consequently (d) an increased intraperitoneal oncotic pressure due to intraperitoneal protein concentration (Tamsma *et al*, 2001). Using the printed glycan array, we observed an unexpectedly rich spectrum of AGA with similar amounts in plasma and ascites. These findings suggested that there is an equilibrium between both body fluids. Early lymphatic obstruction is one of the first manifestations of an inflammatory reaction (Feldman, 1975). As IgM has an important role in inflammation with multivalent antigen binding due to its pentameric structure and as the first immunoglobulin class produced in a primary response to an antigen, lymphatic obstruction may result in a rapid increase in IgM secreting plasma cells. Natural circulating AGA have also been described in various inflammatory conditions, including diabetes mellitus type 1 (Gillard *et al*, 1989), chronic inflammatory bowel and Crohn's disease (Malickova *et al*, 2006) and in patients with cancer (Young *et al*, 1979; Springer, 1984; Springer *et al*, 1988; Desai *et al*, 1995).

We also investigated the expression of *A4GALT* P$_1$- and P^k-profiled cell lines. As seen in our study, *A4GALT* is overexpressed in the P$_1$- and P^k-positive ovarian cancer cell line IGROV1 (Jacob *et al*, 2011b), suggesting that *A4GALT* is not only involved in P^k but also in P$_1$ synthesis in ovarian cancer cells. We propose that *A4GALT* is involved in the progression of various ovarian and peritoneal cancers; however, the molecular link between *A4GALT* mRNA levels and P$_1$ expression remains unknown. This is consistent with suspension array results in which no tested clinical parameters were shown to correlate with lower AGA levels to P$_1$ trisaccharide. A recently identified single nucleotide polymorphism

(CT conversion) encoding an additional exon in the genomic region of *A4GALT* (Thuresson *et al*, 2011) could probably explain the presence of P$_1$ in cancer cells. However, it is unclear whether the overexpression of *A4GALT* is causative for the synthesis of P$_1$ or P^k in profiled cancer cell lines. The invasive phenotype of colon cells lacking P^k could be induced and inhibited by the transfection of Gb3 synthase (*A4GALT*) or RNA interference, respectively (Kovbasnjuk *et al*, 2005). Another immunohistochemistry-based study showed that P^k expression was elevated in colorectal cancers and their metastases; however, *A4GALT* mRNA levels, protein expression or galactosyltransferase activity were not investigated (Falguieres *et al*, 2008). The potential role of A4GALT in cancer initiation or progression needs to be elucidated in future studies with respect to all P blood group-related glycans.

For the first time, we also observed migration rate in P$_1$-high-expressing cells, and this was even more obvious when araC, a proliferation inhibitor, was added to the cultures (Roy *et al*, 2006). The addition of araC confirmed that the observed difference in migration was indeed due to altered cell migration and not cell proliferation. Our results suggest an involvement of P$_1$ in cell migration, but the underlying molecular mechanisms are unknown.

Finally, this study provides further evidence that P blood group-related antigens have a role in carcinogenesis and those naturally occurring anti-glycan IgM antibodies against them may have the potential to discriminate ovarian cancer patients from healthy individuals. If these surface antigens prove to be indeed tumour-specific, they may become candidate molecular targets for potential imaging tools for confocal fluorescence endoscopy and positron emission tomography and as tools in targeted immunotherapy (Janssen *et al*, 2006; Viel *et al*, 2008).

REFERENCES

Boes M (2000) Role of natural and immune IgM antibodies in immune responses. *Mol Immunol* **37**(18): 1141–1149.

Bovin N, Obukhova P, Shilova N, Rapoport E, Popova I, Navakouski M, Unverzagt C, Vuskovic M, Huflejt M (2012) Repertoire of human natural anti-glycan immunoglobulins. Do we have auto-antibodies? *Biochim Biophys Acta* **1820**(9): 1373–1382.

Bovin NV (2013) Natural antibodies to glycans. *Biochemistry (Moscow)* **78**(7): 786–797.

Brandlein S, Beyer I, Eck M, Bernhardt W, Hensel F, Muller-Hermelink HK, Vollmers HP (2003) Cysteine-rich fibroblast growth factor receptor 1, a new marker for precancerous epithelial lesions defined by the human monoclonal antibody PAM-1. *Cancer Res* **63**(9): 2052–2061.

Brandlein S, Eck M, Strobel P, Wozniak E, Muller-Hermelink HK, Hensel F, Vollmers HP (2004a) PAM-1, a natural human IgM antibody as new tool for detection of breast and prostate precursors. *Hum Antibodies* **13**(4): 97–104.

Brandlein S, Pohle T, Vollmers C, Wozniak E, Ruoff N, Muller-Hermelink HK, Vollmers HP (2004b) CFR-1 receptor as target for tumor-specific apoptosis induced by the natural human monoclonal antibody PAM-1. *Oncol Rep* **11**(4): 777–784.

Chai W, Piskarev V, Lawson AM (2001) Negative-ion electrospray mass spectrometry of neutral underivatized oligosaccharides. *Anal Chem* **73**(3): 651–657.

Chang WW, Lee CH, Lee P, Lin J, Hsu CW, Hung JT, Lin JJ, Yu JC, Shao LE, Yu J, Wong CH, Yu AL (2008) Expression of Globo H and SSEA3 in breast cancer stem cells and the involvement of fucosyl transferases 1 and 2 in Globo H synthesis. *Proc Natl Acad Sci USA* **105**(33): 11667–11672.

Chmiela M, Wadstrom T, Folkesson H, Planeta Malecka I, Czkwianianc E, Rechcinski T, Rudnicka W (1998) Anti-Lewis X antibody and Lewis X-anti-Lewis X immune complexes in *Helicobacter pylori* infection. *Immunol Lett* **61**(2-3): 119–125.

Desai PR, Ujjainwala LH, Carlstedt SC, Springer GF (1995) Anti-Thomsen-Friedenreich (T) antibody-based ELISA and its application to human breast carcinoma detection. *J Immunol Methods* **188**(2): 175–185.

Desselle A, Chaumette T, Gaugler MH, Cochonneau D, Fleurence J, Dubois N, Hulin P, Aubry J, Birkle S, Paris F (2012) Anti-gb3 monoclonal antibody inhibits angiogenesis and tumor development. *PLoS One* **7**(11): e45423.

Domon B, Costello CE (1988) Structure elucidation of glycosphingolipids and gangliosides using high-performance tandem mass spectrometry. *Biochemistry* **27**(5): 1534–1543.

Everest-Dass AV, Jin D, Thaysen-Andersen M, Nevalainen H, Kolarich D, Packer NH (2012) Comparative structural analysis of the glycosylation of salivary and buccal cell proteins: innate protection against infection by *Candida albicans*. *Glycobiology* **22**(11): 1465–1479.

Falguieres T, Maak M, von Weyhern C, Sarr M, Sastre X, Poupon MF, Robine S, Johannes L, Janssen KP (2008) Human colorectal tumors and metastases express Gb3 and can be targeted by an intestinal pathogen-based delivery tool. *Mol Cancer Ther* **7**(8): 2498–2508.

Feldman GB (1975) Lymphatic obstruction in carcinomatous ascites. *Cancer Res* **35**(2): 325–332.

Gilewski T, Ragupathi G, Bhuta S, Williams LJ, Musselli C, Zhang XF, Bornmann WG, Spassova M, Bencsath KP, Panageas KS, Chin J, Hudis CA, Norton L, Houghton AN, Livingston PO, Danishefsky SJ (2001) Immunization of metastatic breast cancer patients with a fully synthetic globo H conjugate: a phase I trial. *Proc Natl Acad Sci USA* **98**(6): 3270–3275.

Gillard BK, Thomas JW, Nell LJ, Marcus DM (1989) Antibodies against ganglioside GT3 in the sera of patients with type I diabetes mellitus. *J Immunol* **142**(11): 3826–3832.

Gupta V, Bhinge KN, Hosain SB, Xiong K, Gu X, Shi R, Ho MY, Khoo KH, Li SC, Li YT, Ambudkar SV, Jazwinski SM, Liu YY (2012) Ceramide glycosylation by glucosylceramide synthase selectively maintains the properties of breast cancer stem cells. *J Biol Chem* **287**(44): 37195–37205.

Hakomori S (1998) Cancer-associated glycosphingolipid antigens: their structure, organization, and function. *Acta Anat* **161**(1-4): 79–90.

Hakomori S, Wang SM, Young Jr. WW (1977) Isoantigenic expression of Forssman glycolipid in human gastric and colonic mucosa: its possible identity with "A-like antigen" in human cancer. *Proc Natl Acad Sci USA* **74**(7): 3023–3027.

Hakomori SI (2010) Glycosynaptic microdomains controlling tumor cell phenotype through alteration of cell growth, adhesion, and motility. *FEBS Lett* **584**(9): 1901–1906.

Huflejt ME, Vuskovic M, Vasiliu D, Xu H, Obukhova P, Shilova N, Tuzikov A, Galanina O, Arun B, Lu K, Bovin N (2009) Anti-carbohydrate antibodies of normal sera: findings, surprises and challenges. *Mol Immunol* **46**(15): 3037–3049.

Jacob F, Goldstein DR, Bovin NV, Pochechueva T, Spengler M, Caduff R, Fink D, Vuskovic MI, Huflejt ME, Heinzelmann-Schwarz V (2012) Serum antiglycan antibody detection of nonmucinous ovarian cancers by using a printed glycan array. *Int J Cancer* **130**(1): 138–146.

Jacob F, Meier M, Caduff R, Goldstein D, Pochechueva T, Hacker N, Fink D, Heinzelmann-Schwarz V (2011a) No benefit from combining HE4 and CA125 as ovarian tumor markers in a clinical setting. *Gynecol Oncol* **121**(3): 487–491.

Jacob F, Tse BWC, Guertler R, Nixdorf S, Bovin NV, Hacker N, Heinzelmann-Schwarz V (2011b) P1 antigen is present on the serous ovarian cancer cell line, IGROV1, correlating with A4GALT overexpression and altered cell behaviour. *Glycobiology* **21**(11): 1454–1531.

Janssen KP, Vignjevic D, Boisgard R, Falguieres T, Bousquet G, Decaudin D, Dolle F, Louvard D, Tavitian B, Robine S, Johannes L (2006) In vivo tumor targeting using a novel intestinal pathogen-based delivery approach. *Cancer Res* **66**(14): 7230–7236.

Jarvis WD, Grant S, Kolesnick RN (1996) Ceramide and the induction of apoptosis. *Clin Cancer Res* **2**(1): 1–6.

Johansson D, Andersson C, Moharer J, Johansson A, Behnam-Motlagh P (2010) Cisplatin-induced expression of Gb3 enables verotoxin-1 treatment of cisplatin resistance in malignant pleural mesothelioma cells. *Br J Cancer* **102**(2): 383–391.

Karlsson H, Halim A, Teneberg S (2010) Differentiation of glycosphingolipid-derived glycan structural isomers by liquid chromatography/mass spectrometry. *Glycobiology* **20**(9): 1103–1116.

Kasahara K, Sanai Y (1999) Possible roles of glycosphingolipids in lipid rafts. *Biophys Chem* **82**(2-3): 121–127.

Ke N, Wang X, Xu X, Abassi YA (2011) The xCELLigence system for real-time and label-free monitoring of cell viability. *Methods Mol Biol* **740**: 33–43.

Kovbasnjuk O, Mourtazina R, Baibakov B, Wang T, Elowsky C, Choti MA, Kane A, Donowitz M (2005) The glycosphingolipid globotriaosylceramide in the metastatic transformation of colon cancer. *Proc Natl Acad Sci USA* **102**(52): 19087–19092.

Lavoue V, Thedrez A, Leveque J, Foucher F, Henno S, Jauffret V, Belaud-Rotureau MA, Catros V, Cabillic F (2013) Immunity of human epithelial ovarian carcinoma: the paradigm of immune suppression in cancer. *J Transl Med* **11**: 147.

Li J, Lee AS (2006) Stress induction of GRP78/BiP and its role in cancer. *Curr Mol Med* **6**(1): 45–54.

Malickova K, Lukas M, Donoval R, Sandova P, Janatkova I (2006) Novel anti-carbohydrate autoantibodies in patients with inflammatory bowel disease: are they useful for clinical practice? *Clin Lab* **52**(11-12): 631–638.

Martin F, Kearney JF (2001) B1 cells: similarities and differences with other B cell subsets. *Curr Opin Immunol* **13**(2): 195–201.

Oyelaran O, McShane LM, Dodd L, Gildersleeve JC (2009) Profiling human serum antibodies with a carbohydrate antigen microarray. *J Proteome Res* **8**(9): 4301–4310.

Ozols RF (2006) Challenges for chemotherapy in ovarian cancer. *Ann Oncol* **17**(Suppl 5): v181–v187.

Panjwani N, Zhao Z, Ahmad S, Yang Z, Jungalwala F, Baum J (1995) Neolactoglycosphingolipids, potential mediators of corneal epithelial cell migration. *J Biol Chem* **270**(23): 14015–14023.

Pochechueva T, Chinarev A, Spengler M, Korchagina E, Heinzelmann-Schwarz V, Bovin N, Rieben R (2011a) Multiplex suspension array for human anti-carbohydrate antibody profiling. *Analyst* **136**(3): 560–569.

Pochechueva T, Jacob F, Fedier A, Heinzelmann-Schwarz V (2012) Tumor-associated glycans and their role in gynecological cancers: accelerating translational research by novel-high throughput approaches. *Metabolites* **2**(4): 913–939.

Pochechueva T, Jacob F, Goldstein DR, Huflejt ME, Chinarev A, Caduff R, Fink D, Hacker N, Bovin NV, Heinzelmann-Schwarz V (2011b) Comparison of printed glycan array, suspension array and ELISA in the detection of human anti-glycan antibodies. *Glycoconj J* **28**(8-9): 507–517.

Pohle T, Brandlein S, Ruoff N, Muller-Hermelink HK, Vollmers HP (2004) Lipoptosis: tumor-specific cell death by antibody-induced intracellular lipid accumulation. *Cancer Res* **64**(11): 3900–3906.

Robbe C, Capon C, Coddeville B, Michalski JC (2004) Diagnostic ions for the rapid analysis by nano-electrospray ionization quadrupole time-of-flight mass spectrometry of O-glycans from human mucins. *Rapid Commun Mass Spectrom* **18**(4): 412–420.

Rodriguez-Zhurbenko N, Martinez D, Blanco R, Rondon T, Grinan T, Hernandez AM (2013) Human antibodies reactive to NeuGcGM3 ganglioside have cytotoxic antitumor properties. *Eur J Immunol* **43**(3): 826–837.

Roy AM, Tiwari KN, Parker WB, Secrist 3rd JA, Li R, Qu Z (2006) Antiangiogenic activity of 4'-thio-beta-D-arabinofuranosylcytosine. *Mol Cancer Ther* **5**(9): 2218–2224.

Solly K, Wang X, Xu X, Strulovici B, Zheng W (2004) Application of real-time cell electronic sensing (RT-CES) technology to cell-based assays. *Assay Drug Dev Technol* **2**(4): 363–372.

Springer GF (1984) T and Tn, general carcinoma autoantigens. *Science* **224**(4654): 1198–1206.

Springer GF, Chandrasekaran EV, Desai PR, Tegtmeyer H (1988) Blood group Tn-active macromolecules from human carcinomas and erythrocytes: characterization of and specific reactivity with mono- and poly-clonal

anti-Tn antibodies induced by various immunogens. *Carbohydr Res* **178**: 271.

Tamsma JT, Keizer HJ, Meinders AE (2001) Pathogenesis of malignant ascites: Starling's law of capillary hemodynamics revisited. *Ann Oncol* **12**(10): 1353–1357.

Taniguchi N, Yokosawa N, Narita M, Mitsuyama T, Makita A (1981) Expression of Forssman antigen synthesis and degradation in human lung cancer. *J Natl Cancer Inst* **67**(3): 577–583.

Thuresson B, Westman JS, Olsson ML (2011) Identification of a novel A4GALT exon reveals the genetic basis of the P1/P2 histo-blood groups. *Blood* **117**(2): 678–687.

Todeschini AR, Dos Santos JN, Handa K, Hakomori SI (2008) Ganglioside GM2/GM3 complex affixed on silica nanospheres strongly inhibits cell motility through CD82/cMet-mediated pathway. *Proc Natl Acad Sci USA* **105**(6): 1925–1930.

Viau M, Zouali M (2005) B-lymphocytes, innate immunity, and autoimmunity. *Clin Immunol* **114**(1): 17–26.

Viel T, Dransart E, Nemati F, Henry E, Theze B, Decaudin D, Lewandowski D, Boisgard R, Johannes L, Tavitian B (2008) In vivo tumor targeting by the B-subunit of shiga toxin. *Mol Imaging* **7**(6): 239–247.

Vollmers HP, Brandlein S (2007) Natural antibodies and cancer. *J Autoimmun* **29**(4): 295–302.

Wang CC, Huang YL, Ren CT, Lin CW, Hung JT, Yu JC, Yu AL, Wu CY, Wong CH (2008) Glycan microarray of Globo H and related structures for quantitative analysis of breast cancer. *Proc Natl Acad Sci USA* **105**(33): 11661–11666.

Wenk J, Andrews PW, Casper J, Hata J, Pera MF, von Keitz A, Damjanov I, Fenderson BA (1994) Glycolipids of germ cell tumors: extended globo-series glycolipids are a hallmark of human embryonal carcinoma cells. *Int J Cancer* **58**(1): 108–115.

Young Jr. WW, Hakomori SI, Levine P (1979) Characterization of anti-Forssman (anti-Fs) antibodies in human sera: their specificity and possible changes in patients with cancer. *J Immunol* **123**(1): 92–96.

Supplementary Information accompanies this paper on British Journal of Cancer website (http://www.nature.com/bjc)